Journal of Physics: Conference Series

PAPER • **OPEN ACCESS**

The PADME electromagnetic calorimeter

To cite this article: Gabriele Piperno and PADME collaboration 2019 *J. Phys.: Conf. Ser.* **1162** 012031

View the article online for updates and enhancements.

IOP ebooks™

Bringing you innovative digital publishing with leading voices to create your essential collection of books in STEM research.

Start exploring the collection - download the first chapter of every title for free.

This content was downloaded from IP address 141.108.32.152 on 18/12/2019 at 11:05

IOP Conf. Series: Journal of Physics: Conf. Series 1162 (2019) 012031 doi:10.1088/1742-6596/1162/1/012031

The PADME electromagnetic calorimeter

Gabriele Piperno[a,b] for the PADME collaboration[1]

[a]Dipartimento di Fisica, Sapienza Università di Roma, I 00185 Roma, Italy
[b]INFN, Sezione di Roma, I 00185 Roma, Italy

E-mail: gabriele.piperno@roma1.infn.it

Abstract.
The PADME experiment, hosted at Laboratori Nazionali di Frascati in Italy, is going to start its data taking in September 2018. It is designed to search for the Dark Photon (indicated by the symbol A'), an hypothetical particle that can explain the Dark Matter elusiveness, possibly produced in the reaction $e^+ e^- \to A' \gamma$. Together with the target, the segmented electromagnetic calorimeter is the most important component of the experiment, since it is needed to detect the recoil photon energy and position, in such a way to measure the A' mass. It will consist of 616 $2.1 \times 2.1 \times 23.0\,\mathrm{cm}^3$ BGO crystals arranged in a cylindrical shape and read by HZC photomultipliers with a diameter of 1.9 cm. Here we present the results obtained during the measurements performed on the scintillating units with a radioactive source and test beams, together with an overall description of the entire experiment.

1. Introduction

Many decades of experimental observations suggest that the 27% of the Universe density components are made of a non-baryonic and non-luminous form of matter, that, for this reason, is called Dark Matter (DM) [1]. Despite all these indications, its real nature is still unknown.

A possible explanation of its detection elusiveness is that DM lives in a separated sector with respect the Standard Model (SM), the so called Dark Sector (DS), and interacts with it only by means of portals. One of the simplest portals only consists of a new U(1) symmetry, that comes with its vector boson, the Dark Photon (DP), indicated with the symbol A'. SM particles are neutral under this symmetry, while the DP could interact with them thanks to a faint mixing with the ordinary photon. This will result in an effective charge εe, where e is the electric charge of the SM particle and ε is the A' coupling constant.

The simplicity of this model allows it to be extremely predictive and reflects in the need to add only the new constant ε and the DP mass $m_{A'}$ to describe the A' completely.

In addition to this, depending on the selected model (for a more complete scenario see [2, 3]), the DP can explain partially or completely the discrepancy between the expected and

[1] G. Chiodini, P. Creti, F. Oliva, V. Scherini (INFN Lecce); A.P. Caricato, M. Martino, G. Maruccio, A. Monteduro, S. Spagnolo (INFN Lecce e Dip. di Matematica e Fisica, Università del Salento); P. Albicocco, R. Bedogni, F. Bossi, B. Buonomo, R. de Sangro, G. Finocchiaro, L.G. Foggetta, A. Ghigo, P. Gianotti, M. Palutan, I. Sarra, B. Sciascia, T. Spadaro, E. Spiriti, C. Taruggi, E. Vilucchi (INFN Laboratori Nazionali di Frascati); F. Ameli, F. Ferrarotto, E. Leonardi, F. Safai Tehrani, P. Valente (INFN Roma1); S. Fiore (INFN Roma1 e ENEA); G.C. Organtini, M. Raggi (INFN Roma1 e Dip. di Fisica, "Sapienza" Università di Roma); L. Tsankov (University of Sofia "St. Kl. Ohridski"); G. Georgiev, V. Kozhuharov (University of Sofia "St. Kl. Ohridski" and INFN Laboratori Nazionali di Frascati).

Content from this work may be used under the terms of the Creative Commons Attribution 3.0 licence. Any further distribution of this work must maintain attribution to the author(s) and the title of the work, journal citation and DOI.
Published under licence by IOP Publishing Ltd

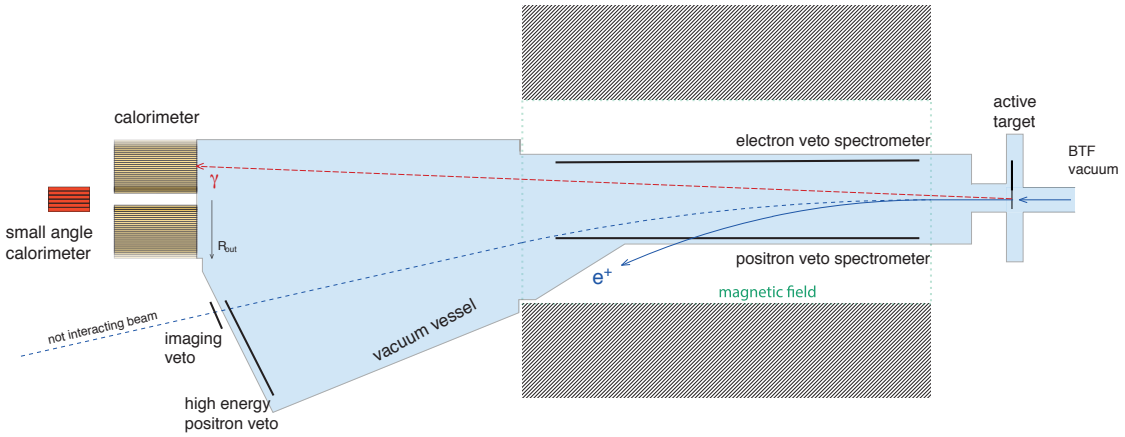

Figure 1. PADME detector schematics, from right to left: diamond active target, magnetic dipole (0.5 T, 1 m length and 23 cm gap) with electron/positron vetoes inside, high energy positron veto close to the beam exit, ECAL (a $\sim$ 30 cm radius cylinder of 616 scintillating BGO crystals with a central square hole, placed at 3 m from the target) and SAC (25 PbF_2 crystals, arranged in a square shape of 15 cm side and based on Cherenkov light detection).

the measured value of the muon anomalous magnetic moment $(g-2)_\mu$ [4] and the observation currently known as the "Beryllium-8 anomaly" [5].

The DP decays can be divided into two classes: visible decays and invisible decays. First case is when there are no DM particles with mass $m_{DM} \leq m_{A'}/2$ and the A' is forced to decay into SM particle, while the latter is when DM particles with $m_{DM} \leq m_{A'}/2$ do exist and the A' will predominantly decay into them, suppressing by a factor ε^2 the SM decays.

2. The PADME experiment

PADME (Positron Annihilation into Dark Matter Experiment) is hosted at the Laboratori Nazionali di Frascati (LNF) in Italy and is designed to search for a DP that decays into invisible, looking for the reaction

$$e^+ e^- \rightarrow A' \gamma,$$

where the positron comes from the 550 MeV LNF linear accelerator and the electron from a diamond active target. If produced, the A' will leave the experiment undetected, while the γ can be observed by means of a electromagnetic calorimeter. Hence, knowing the initial conditions for the interacting e^+ and e^- ($\vec{P}_{e^+}$, 550 MeV in the beam direction and $\vec{P}_{e^-} = \vec{0}$) and measuring the γ in the final state ($\vec{P}_\gamma$) it is possible to evaluate the DP mass as the detector missing mass M_{miss} using the formula (underlined indicate the relativistic four-momentum):

$$M^2_{miss} = \left(\underline{P}_{e^-} + \underline{P}_{e^+} - \underline{P}_\gamma\right)^2.$$

It is important to highlight that with this experimental approach there are only minimal model dependent assumptions on the DP: it is only required that it interacts with leptons.

Following fig.1 from right to left, the detector is compose of following elements:

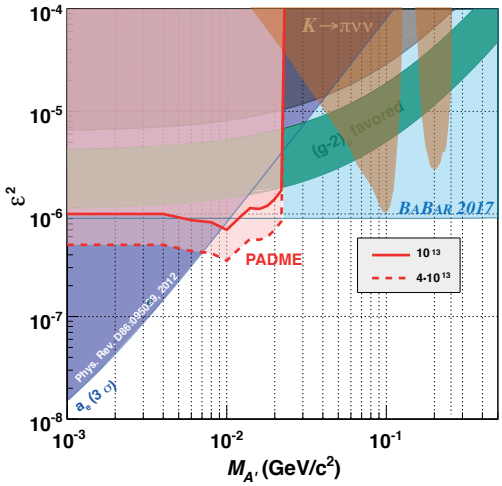

Figure 2. PADME sensitivity for a DP that decays into DS particles for two different statistics of 10^{13} and $4 \cdot 10^{13}$ positrons on target.

- Active target. A $2 \times 2\,\mathrm{cm}^2$ area and $100\,\mu\mathrm{m}$ thickness diamond target with 19 horizontal and vertical graphitic stripes, to obtain average informations about beam intensity and position (resolution $\approx 5\,\mathrm{mm}$). The material is carbon to reduce the bremsstrahlung cross section, while the small thickness is to lower the positron multiple interactions.
- Magnetic dipole. Placed 20 cm after the target, a large-gap dipole magnet (a spare bending from the SPS transfer-line) to bend the positrons that did not interact with the target towards a dump and to send the ones that lost energy due to bremsstrahlung to the vetoes.
- Veto for electrons and (high energy) positrons. It consists of two parts, one inside the magnet (1 m long), to detect electrons and positrons produced in $e^+\,e^- \to e^+\,e^-$ interaction or positrons that lost a huge amount of their energy for bremsstrahlung, the other close to the beam exit (36 cm long), to identify positrons that lost only a small amount of energy for bremsstrahlung. Both are made of $1 \times 1 \times 16\,\mathrm{cm}^3$ plastic scintillator bars.
- Electromagnetic calorimeter (ECAL). Positioned at 3 m from the target, it is composed of 616 bismuth germanate (BGO) crystals, each of $2.1 \times 2.1 \times 23.0\,\mathrm{cm}^3$, displaced in a cylindrical shape of 29 cm radius with a central square hole to let the bremsstrahlung photons pass and be observed by a faster small angle calorimeter. This is needed because the decay time of the BGO scintillation light (300 ns) is too long for the bremsstrahlung expected rate. Expected time, space and energy resolutions are 700 ps, 5 mm and $2\%/\sqrt{E}$ [6], respectively.
- Small Angle Calorimeter (SAC). This detector is made of 25 $3 \times 3 \times 14\,\mathrm{cm}^3$ lead difluoride (PbF_2) crystals arranged in a square shape and it is located immediately behind the ECAL. Being based on Cherenkov light its dead time is of ≈ 3 ns and, hence, it is able to cope with event rates higher than the ECAL ones.

An $e^+\,e^- \to A'\,\gamma$ event in the detector would appear as an unbalanced reaction (the missing energy taken away from the A') with a single γ in the ECAL and no hits in SAC or vetoes. With a beam energy of 550 MeV the maximum A' mass that can be probed is 23.7 MeV.

In fig.2 it is presented the PADME sensitivity to an invisibly decaying A' for a statistics of 10^{13} and $4 \cdot 10^{13}$ positrons on target and assuming as DP model the simple one presented in the previous section.

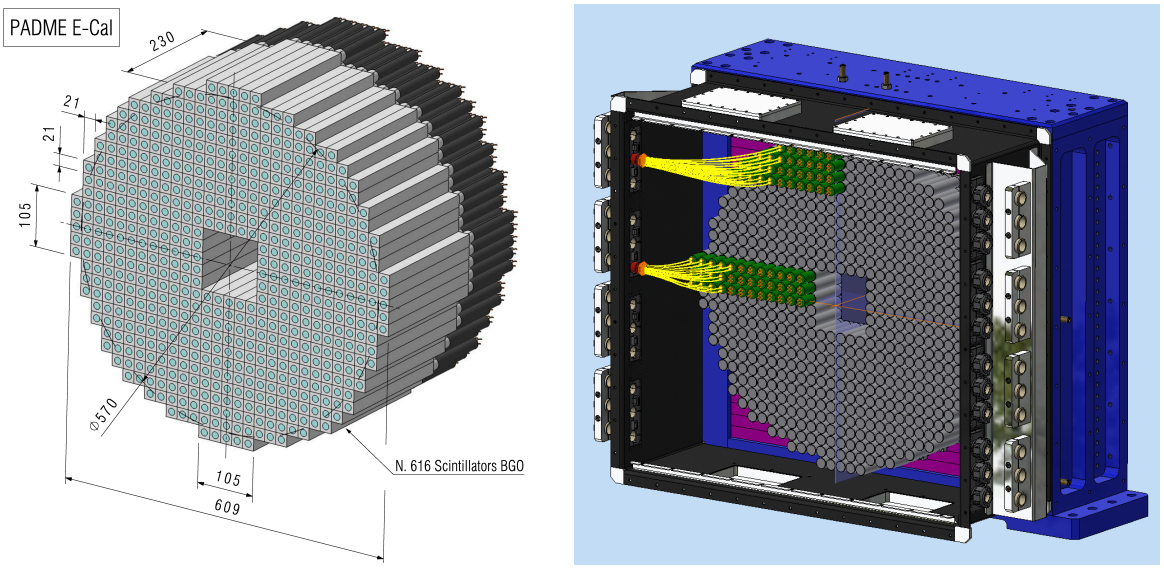

Figure 3. Left: render of the PADME ECAL SUs displacement, seen from the front. Right: PADME ECAL seen from behind with its mechanical support; for sake of clarity only some PMT dividers and signal and HV cables are shown.

3. Scintillating units for the electromagnetic calorimeter

The calorimeter crystals have been recuperated from one of the endcaps of the electromagnetic calorimeter of the decommissioned L3 experiment at LEP [7]. After paint and photosensor removal, to recover a possible degradation of the performances, due to the loss of transparency induced by radiation, they underwent an accelerated annealing procedure at LAB27 at CERN through a high-temperature cycle:

(i) from room temperature up to 200 °C in 3 h;
(ii) constant temperature at 200 °C for 6 h;
(iii) turn off the oven and let the crystals reach room temperature.

After the annealing, the BGO have been cut to the final shape (starting from the truncated pyramid original one), polished, glued together with the photosensors and painted. All these steps have been performed at Gestione SILO [8], a firm close to Firenze, Italy. The used glue is the ELJEN optical cement EJ-500 [9], while crystal are covered with three layers ($\approx 60\,\mu$m) of reflective paint ELJEN EJ-510 [10].

The selected photosensors are the XP1911 type B photomultipliers (PMTs) from HZC Photonics [11], which wavelength acceptance window well matches the BGO emission spectrum, that has a maximum at 480 nm. Before being selected for gluing, each photomultiplier has been tested with a pulsing blue LED at different voltages, to check its working and to measure its gain curve.

3.1. PADME electromagnetic calorimeter

A sketch of the PADME electromagnetic calorimeter is presented in fig.3. On the left there is only the SUs displacement seen from the front, while on the right there is all the support structure and the PMTs enclosure seen from behind. As can be seen the circular shape is inserted inside a square one, which is easier to machine. The coupling between the two is done by mean of plastic fillers, visible in violet in fig.3 right, that also ensure a lower budget material,

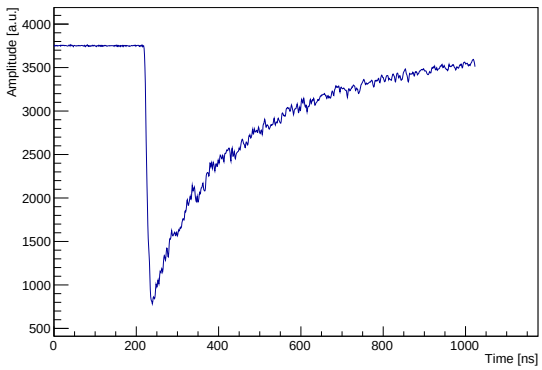

Figure 4. An example of a pulse coming from a SU and digitized at 1 GS/s by the V1742 CAEN board.

with respect to the metal, in contact with the BGO. Here are shown as well some PMT dividers, in green, and some HV and signal cables, in yellow. All the cables exit in groups of 64 passing through two holders, the inner of which is also light-tight.

All the layers are assembled selecting crystals of the same height to ensure a flat base for the subsequent floor. In addition, to avoid optical crosstalk, all the crystals are separated by means of 50 μm tedlar black foils: with a strip between side by side crystals and with a sheet between layers, both with dimensions to completely cover the facing surfaces.

3.2. Calorimeter redout

The analog signal that arrives from the detector is digitized using CAEN V1742 boards. Every board has 32 channels distributed on four DSR4 chips. Each channel is 12 bit with 1 V peak-to-peak maximum amplitude, used in the range $[-1, 0]$ V, because of the PMTs negative signals.

The CAEN V1742 has 1024 samples for each of the 32 channel and allows to select among three different sampling frequencies: 1 GS/s, 2.5 GS/s and 5 GS/s. Given the long decay time of the BGO scintillation light, the selected one is 1 GS/s, in such a way to have about 3 decay times for a pulse in a triggered window (about 200 ns are taken to evaluate the baseline). In fig.4 it is shown a typical SU digitized pulse that, time integrated, gives an indication about the energy released inside the crystal.

4. Test results

In [6] are presented some results obtained with a 5×5 pre-production crystals matrix on a variable energy electron beam at the Beam-Test Facility. The fit to the energy resolution with the function

$$\frac{\sigma(E)}{E} = \frac{a}{\sqrt{E[\mathrm{GeV}]}} \oplus \frac{b}{E[\mathrm{GeV}]} \oplus c$$

gives the following parameters: $a = 2.0\%$, $b = 0.003\%$ and $c = 1.1\%$, which are compatible with the L3 results [7]. There, it is studied also the linearity, which remains within the 2% up to 1 GeV.

Other tests have been performed with a ^{22}Na source, exploiting its back-to-back emission of two 511 keV γs. Also in this case, the Scintillating units (SU), composed of the BGO crystal and the photomultiplier, are grouped in 5×5 matrices. The ^{22}Na source is moved in front of each crystal by means of two step motors. On the opposite side of the source with respect to

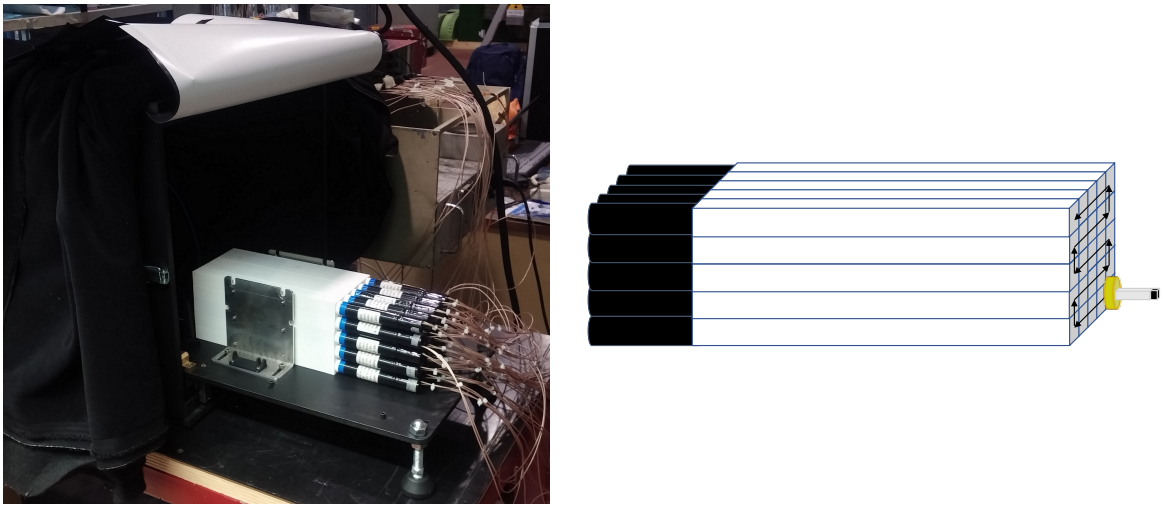

Figure 5. Left: a picture of a 5×5 BGO matrix ready to be covered with a black cover and measured with the ^{22}Na source (not visible). Right: schematics of the ^{22}Na source movements in front of each crystal.

the BGO it is placed a $3 \times 3 \times 20\,\mathrm{mm}^3$ LySO crystal read by a SiPM and used as trigger: when a pulse in this detector exceed a threshold, the SU signal is recorded. For every SU, about 6000 signals are collected at 10 different HV in the range $[1100, 1550]$ V, in steps of 50 V. In fig.5 are shown a picture of the test setup and a schematics of its working principle.

An example of charge spectrum obtained at 1550 V is presented in fig.6 left. Here are clearly visible the pedestal and the 511 keV peaks. To evaluate correctly the 511 keV peak charge, the spectrum is fitted with a double gaussian plus a constant function, to accomodate the background. Then, after the construction of the charge vs HV plot (as in fig.6 right), it is possible to find the voltage for a pC/MeV equalization of all the units. The used fit function is $Q = A \cdot V^s$, where Q is the charge, V is the HV and A and s are the fit parameters.

In fig.7 it is shown the distribution of the 511 keV peak mean for 25 SU equalized at 20 pC/MeV. As visible, two PMTs were not working due to divider problems. The expected mean of the gaussian fit to the working units is 10.22 pC, which is within $1\,\sigma$ from the obtained result of (10.4 ± 0.2) pC and the difference corresponds to less than the 2%.

To evaluate the stability of the results, some SUs have been re-measured with the ^{22}Na source using the same HV steps. In fig.8 left it is presented the curve of the relative difference between the charge in the first (Q_1) and in the second (Q_2) measurement, $(Q_1 - Q_2)/Q_1$, as a function of the voltage, for a single SU. Typically, the relative difference get closer to zero for larger voltages. This is due to the fact that any possible systematics becomes relatively less and less important with the charge increase.

Exploiting the repeated measurement, it is possible to extrapolate a second HV for the pC/MeV equalization and compare it with the result of the first evaluation. In fig.8 right there is the distribution of the relative difference between the two voltages $(HV_{eq,1} - HV_{eq,2})/HV_{eq,1}$ for an equalization of 20 pC/MeV for 25 SU. In this case, the maximum variation is of the order of 1%, which corresponds to about $[11, 13]$ V.

It has to be considered that the repeated measurement differences are due not only to the SU results variability, but also to external conditions, like temperature (BGO light yield depends on the crystal temperature as $-0.9\%/^\circ$C a room temperature) and daylight.

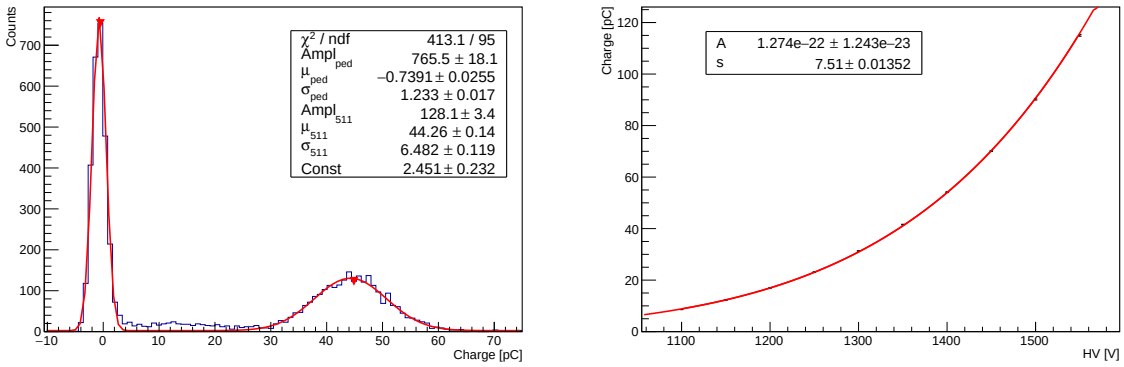

Figure 6. Left: ^{22}Na source charge spectrum obtained with a single SU during the tests at 1550 V, where are visible the pedestal and the 511 keV peaks; the superimposed fit function is given by two gaussians and a flat background. Right: charge vs HV curve for a single SU, only statistical errors are shown.

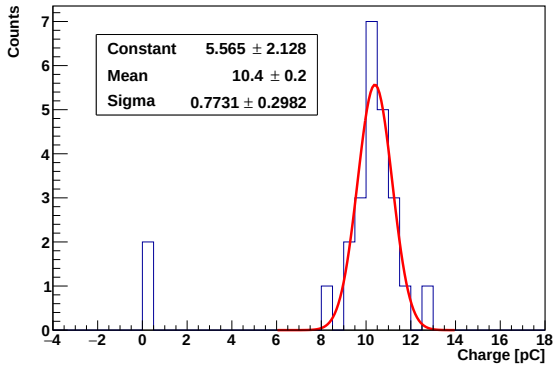

Figure 7. Distribution of the 511 keV peak means for a batch of 25 SU equalized at 20 pC/MeV (the two at 0 pC are not working) with a gaussian fit superimposed. The expected mean, 10.22 pC, is within the error of the obtained result.

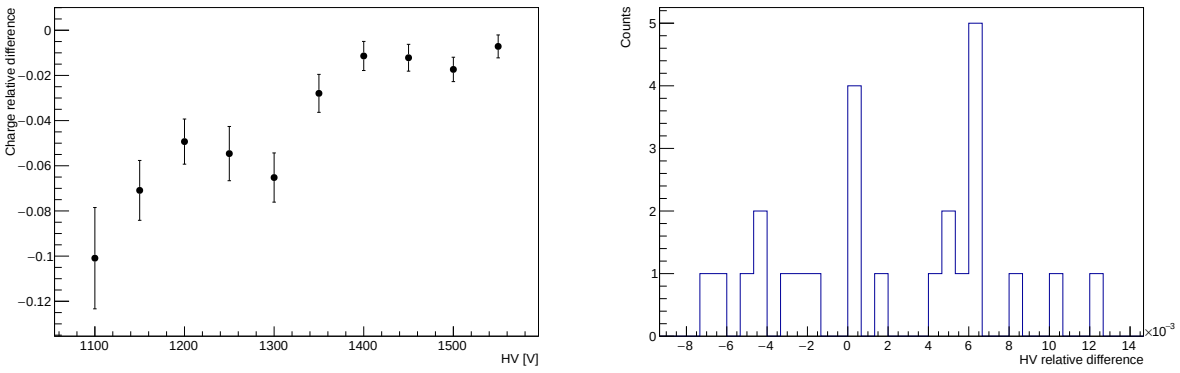

Figure 8. Left: relative difference between the charges of two repeated measurements as a function of the applied voltage for a single SU. Right: distribution of the relative differences between the 20 pC/MeV equalization voltages coming from the two measurements, for 25 SU.

5. Conclusions

PADME is an experiment designed to search for a dark photon possibly produced in the reaction $e^+ e^- \to A' \gamma$, exploiting the 550 MeV positron beam present at the Laboratori Nazionali di Frascati, close to Rome (IT). Its electromagnetic calorimeter consists of 616 $2.1 \times 2.1 \times 23.0\,\mathrm{cm}^3$ BGO scintillating crystals read by mean of photomultipliers. The BGO comes from the L3 electromagnetic calorimeter endcaps and undergone an annealing procedure before being cut, glued with the PMTs and painted. Test beams and measurements with a ^{22}Na radioactive source have been performed to assay their working and their performances.

The energy resolution obtained at the test beam is of the order of $2\%/\sqrt{E[\mathrm{GeV}]}$, compatible with the one from L3. The ^{22}Na results indicate that fitting the charge vs HV trend with a function of the kind $charge = A \cdot (HV)^s$ allows to equalize the pC/MeV with a precision of 2% at 511 keV. Concerning the stability of the results, some of the scintillating units has been measured two times to evaluate the possible differences. The variation on the 20 pC/MeV equalization HV is generally smaller than 1%, hence smaller than a tenth of volts. It is important to underline that all of these results are not corrected for any of the external condition that may change the measurement, like daylight and crystal temperature.

References

[1] Akrami Y *et al.* 2018 *Planck 2018 results. I. Overview and the cosmological legacy of Planck* arXiv:1807.06205
[2] Raggi M and Kozhuharov V 2015 *Riv. Nuovo Cim.* **38** 449
[3] Battaglieri M *et al.* 2015 *US Cosmic Visions: New Ideas in Dark Matter 2017: Community Report* arXiv:1707.04591
[4] Pospelov M 2009 *Phys. Rev.* D **80** 095002
[5] Krasznahorkay A J *et al.* 2016 *Phys. Rev. Lett.* **116** 042501
[6] Raggi M *et al.* 2017 *Nucl. Instrum. Meth.* A **862** 31
[7] Sumner R 1988 *Nucl. Instrum. Meth.* A **265** 252
[8] https://www.gestionesilo.it/
[9] http://www.ggg-tech.co.jp/maker/eljen/ej-500.html
[10] http://www.ggg-tech.co.jp/maker/eljen/ej-510.html
[11] http://www.hzcphotonics.com/